Binary nucleation kinetics: A matrix method

Hanna Vehkamäki, Pentti Paatero, Markku Kulmala, and Ari Laaksonen
Department of Physics, P.O. Box 9, FIN-00014 University of Helsinki, Finland

(Received 11 July 1994; accepted 16 August 1994)

The kinetics of binary nucleation is investigated and an exact method to evaluate the nucleation rate is developed. The exact method accounts for all flows to the stable clusters, and thus the nucleation rate is obtained independently of determining the location of the saddle point in the Gibbs free energy surface. The exact method is based on determination of cluster concentrations, which can be obtained after solving a set of linear equations. The values of the nucleation rate and the direction of flow at the saddle point are calculated for water–sulphuric acid and water–ammonia systems. The results are compared to the results obtained by Stauffer's saddle point integration method for binary nucleation kinetics. The saddle point integration method is found to give a reasonably accurate estimation of nucleation rate in the water–sulphuric acid system. However, in the water–ammonia system the difference is found to be as high as three orders of magnitude. © *1994 American Institute of Physics.*

I. INTRODUCTION

Several theoretical papers concerning binary homogeneous nucleation have appeared in recent years. These papers have mostly concentrated on the energetics of the phenomenon, while the kinetics has received considerably less attention. This is understandable, since variations in factors governing the energetics affect the resulting nucleation rate usually to a much larger extent than variations in the kinetic factors. Consequently, relatively crude approximations of the nucleation kinetics are quite often employed. However, there may be situations in which it is important to describe the kinetics correctly. For instance, when the shape of the free energy surface is relatively flat near the saddle point, the assumptions made in the derivation of the various approximative expressions become questionable.

To date, the most rigorous treatment of binary nucleation kinetics is due to Stauffer,[1] but even his derivation is an approximative one, and holds only in the immediate vicinity of the saddle point. However, recent developments in computer technology have made it possible to solve the exact kinetic equations numerically. In the present paper we developed a matrix method for solving the binary nucleation rate. This method is an extension of well-known summative method in homomolecular nucleation (see, e.g. Ref. 2); below we will refer to it as the exact method. The most significant advantage of the exact method (besides not being restricted to the vicinity of the saddle point) is that one does not have to determine the growth angle nor the Zeldovich factor any more in order to solve the nucleation rate.

The approximative evaluation of the homogeneous nucleation rate in binary vapor systems is based on determining the location of the saddle point in the three-dimensional space $(\Delta G, i, j)$, where ΔG is the Gibbs free-energy of formation of a molecular cluster, and i and j are the numbers of molecules of types a and w in the cluster (e.g., Refs. 3, 4, 5, 6, and 7). The nucleation rate is the number of clusters reaching the free-energy barrier, i.e., becoming capable to grow to larger droplets, in unit time. Since the saddle point corresponds to the minimum height of the free-energy barrier, it is assumed that by far the most important contribution to the nucleation rate comes from the flow through the saddle point. In Stauffer's[1] treatment a saddle point integral method gives an expression to the saddle point flow direction and the nucleation rate. The nucleation rate is a product of three terms, the equilibrium concentration of clusters in saddle point, Zeldovich factor, and average growth rate. However, the saddle point is not always a very sharp minimum of the free-energy barrier, which means that the flow could be significant in quite a large region. One purpose of this work is to check the accuracies of the approximative expressions for the nucleation rate and saddle point flow direction, which are more convenient to use in large (e.g., atmospheric) models. The exact method for solving the binary nucleation rate is not restricted to any particular theory for calculating free energies of molecular clusters. In numerical comparisons we use the classical theory in the form first presented by Doyle[3] as a model of nucleation energetics. However, unlike Doyle, we account for the fact that the free-energy change should be zero for monomers. This is done by applying the so-called self-consistency correction.[8] We are aware of the fact that Doyle's theory is thermodynamically inconsistent in that it assumes the overall mole fraction of the clusters to be the same as the bulk mole fraction, and thus does not take any surface enrichment effects into account.[9] However, at present it is not possible to calculate the free energies of noncritical clusters in a thermodynamically consistent way within the framework of the classical theory.[10] In any case, the free energy model employed is not expected to affect the conclusions concerning nucleation kinetics.

II. THEORY

Completely inelastic (sticking coefficient 1) collisions are used as a model of the nucleation process. The model can be simplified using the assumption that the monomer concentrations are much higher than the concentrations of clusters. Accordingly only the collisions between monomers and clusters are taken into account, and cluster-cluster collisions are neglected due to their relatively low probabilities.

The concentration of clusters containing i molecules of species a and j molecules of species w is $c(i,j)$. It is assumed that clusters with $i>n$ or $j>m$ are immediately removed from the system. This assumption is reasonable, if m and n are large enough for the transition rates from sizes $(n+1,j)$ to (n,j) and $(i,m+1)$ to (i,m) to be negligible.

The net flow $I_w(i,j)$ from cluster size (i,j) to size $(i,j+1)$, and the net flow $I_a(i,j)$ from size (i,j) to size $(i+1,j)$, are defined by,[1]

$$\begin{aligned} I_w(i,j)&=k_w(i,j)c(i,j)-e_w(i,j+1)c(i,j+1),\\ I_a(i,j)&=k_a(i,j)c(i,j)-e_a(i+1,j)c(i+1,j), \end{aligned} \tag{1}$$

where k_w and k_a are the condensation coefficients and e_w and e_a are the evaporation coefficients, for the species a and w, respectively.

The condensation coefficients can be determined using the kinetic gas theory,

$$k_\alpha=c_\alpha\left(\frac{3}{4\pi}\right)^{1/6}(6kT)^{1/2}\left[\frac{1}{m(i,j)}+\frac{1}{m_\alpha}\right]^{1/2} \times[v(i,j)^{1/3}+v_\alpha^{1/3}], \tag{2}$$

where T is temperature, k is Boltzmann's constant, $m(i,j)$ and $v(i,j)$ are the mass and volume of the cluster, and c_α, m_α, and v_α are the concentration, mass, and volume of monomer α, respectively.[11]

The determination of the evaporation coefficients is not as straightforward as with the condensation coefficients. In one-component systems the evaporation coefficients can be calculated assuming that the various cluster sizes obey the Boltzmann distribution in equilibrium conditions. An alternative way of obtaining the evaporation coefficients (independently of any assumptions of cluster distributions) would be using the theory of Nowakowski and Ruckenstein.[12] Their theory is, however, limited to molecules with simple interaction potentials. In binary systems the only alternative so far is to employ the extension of the first of the two methods. Thus, when detailed balance conditions[1]

$$I_w(i,j)=0; \quad I_a(i,j)=0 \quad \forall i,j, \tag{3}$$

hold, the equilibrium concentrations $c^e(i,j)$ follow the Boltzmann distribution

$$c^e(i,j)=F\ \exp\left[\frac{-\Delta G(i,j)}{kT}\right], \tag{4}$$

where

$$F=c(1,0)+c(0,1)+\sum_{i,j} c(i,j)\approx c(1,0)+c(0,1). \tag{5}$$

The evaporation coefficients can be expressed with condensation coefficients and equilibrium concentrations using conditions (3). The solutions are as follows:

$$e_w(i,j)=\frac{k_w(i,j-1)c^e(i,j-1)}{c^e(i,j)} \tag{6}$$

$$e_a(i,j)=\frac{k_a(i-1,j)c^e(i-1,j)}{c^e(i,j)}. \tag{7}$$

Changes of cluster concentrations with time are given by a set of first order differential equations[1]

$$\begin{aligned} \frac{dc(i,j)}{dt}&=e_w(i,j+1)c(i,j+1)+k_w(i,j-1)c(i,j-1)\\ &\quad+e_a(i+1,j)c(i+1,j)+k_a(i-1,j)c(i-1,j)\\ &\quad-[e_w(i,j)+k_w(i,j)+e_a(i,j)+k_a(i,j)]c(i,j), \end{aligned} \tag{8}$$

$$0\leqslant i\leqslant n, \quad 0\leqslant j\leqslant m, \tag{9}$$

$$(i,j)\neq(0,1),(i,j)\neq(1,0). \tag{10}$$

The time derivatives of monomer concentrations are given by equations

$$\frac{dc(0,1)}{dt}=\sum_{i,j} e_w(i,j)c(i,j)-k_w(i,j)c(i,j), \tag{11}$$

$$\frac{dc(1,0)}{dt}=\sum_{i,j} e_a(i,j)c(i,j)-k_a(i,j)c(i,j), \tag{12}$$

In the steady state the monomer concentrations are constant. Consequently, the evaporation and condensation coefficients are also constants, and the differential equations (9) become linear.

Equations (11) and (12) can now be replaced by

$$c(0,1)=c_a, \tag{13}$$

$$c(1,0)=c_w, \tag{14}$$

where c_a and c_w are constants.

The concentrations of clusters of different size can be solved from Eqs. (9), (13), and (14) as functions of time. The number of clusters growing to sizes outside the region limited by m and n in unit time is given by

$$I_{nm}=\sum_{i=0}^{n} k_w(i,m)c(i,m)+\sum_{j=0}^{m} k_a(n,j)c(n,j). \tag{15}$$

If n and m are small, the concentrations on these boundaries will be quite high, and significant transitions from sizes $(n+1,j)$ to (n,j) and $(i,m+1)$ to (i,m) will be ignored. I_{nm} will therefore have a value higher than that of the actual nucleation rate. When the values of n and m are high, the concentrations at the boundaries are near zero, and evaporation from clusters just outside the boundaries does not affect the system (and can therefore be ignored). n and m can be considered large enough when a change in their values does not result in any appreciable change in I_{nm}. In these conditions I_{nm} is equal to the nucleation rate.

In steady-state the left-hand sides of Eqs. (9) are equal to zero. Consequently, Eqs. (9), (13), and (14) form a set of $(m+1)\times(n+1)$ ordinary linear equations, which can be expressed in a matrix form

$$\mathbf{Ac}=\mathbf{b}. \tag{16}$$

The elements of matrix $\mathbf{A}$ are

$$A_{k,k}=-[k_w(i,j)+k_a(i,j)+e_w(i,j)+e_a(i,j)],$$

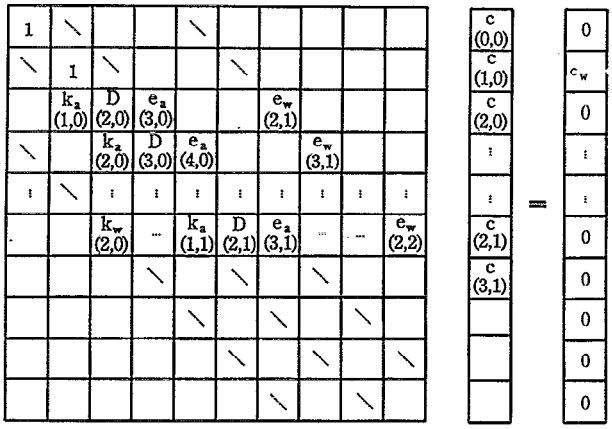

FIG. 1. The set of equations for steady-state concentrations in matrix form. $D(i,j)=-[e_w(i,j)+k_w(i,j)+e_a(i,j)+k_a(i,j)]$.

$$
\begin{aligned}
&A_{k,k-n-1}=k_w(i,j-1),\\
&A_{k,k+n+1}=e_w(i,j+1),\\
&A_{k,k-1}=k_a(i-1,j),\\
&A_{k,k+1}=e_a(i+1,j),\\
&A_{1,1}=1, \quad A_{1,k}=0, \quad \text{when } k\neq 1,\\
&A_{2,2}=1, \quad A_{2,k}=0, \quad \text{when } k\neq 2,\\
&A_{n+2,n+2}=1, \quad A_{n+2,k}=0, \quad \text{when } k\neq n+2,
\end{aligned}
\tag{17}
$$

where $k=j\cdot(n+1)+i+1$, and the components of vectors **c** and **b** are

$$
\begin{aligned}
&c_k=c(i,j),\\
&b_2=c_w,\\
&b_{n+2}=c_a,\\
&b_k=0, \quad \text{when } k\neq 1,2,n+2.
\end{aligned}
\tag{18}
$$

A is a sparse band matrix with nonzero elements only in five bands (Fig. 1). The number of zero bands between the first sub- and superdiagonal and the distant nonzero bands is $n-1$.

The saddle point flow direction is given by

$$\tan\phi=I_w^*/I_a^*, \tag{19}$$

where the flows can be calculated from Eq. (1), and the superscript * refers to the saddle point in the Gibbs free energy surface.

The above description gives exact values for binary nucleation kinetics for a given set of $\Delta G(i,j)$, $i<n, j<m$, when the assumption of constant monomer concentrations hold. Note, that the exact method is in no way dependent on how the cluster free-energies are calculated, and can thus be used together with thermodynamical as well as microphysical free-energy models.

Setting $n=0$ ($m=0$) produces the limiting homomolecular system for $w(a)$. The homomolecular nucleation rate for w is given by

$$
\begin{aligned}
I_m=k_w(0,m)c(0,m)=k_w(0,j)c(0,j)-e_w(0,j+1)\\
\times c(0,j+1)=I_w(0,j),
\end{aligned}
\tag{20}
$$

which is independent of the value of j.

The concentrations can be solved numerically, e.g., by using the NAG-library FORTRAN-routine F07BDF.[13]

Note that the model is analogous to a resistor network, the flows between different clusters corresponding to the electric currents, the Gibbs free-energy corresponding to the potential, and the combination of the evaporation and condensation coefficients corresponding to the resistances.

III. NUMERICAL RESULTS

The nucleation rate and the saddle point flow direction were evaluated by both the exact method and Stauffer's[1] saddle point integration method in H_2O–H_2SO_4 and H_2O–NH_3 systems. The coordinates of the saddle point were defined graphically from the Gibbs free energy surface.

In the numerical comparison we used the self-consistent form for the Gibbs free-energy change ΔG.[8] This ensures $\Delta G=0$ for monomers (which is required for monomer evaporation coefficients to vanish). Thus,

$$
\begin{aligned}
\Delta G=-[j-(1-X)]kT\ln\frac{A_{wg}}{A_{wl}}-(i-X)kT\ln\frac{A_{ag}}{A_{al}}\\
+(36\pi)^{1/3}\sigma\{(iv_a+jv_w)^{2/3}\\
-[(1-X)v_w+Xv_a]^{2/3}\}.
\end{aligned}
\tag{21}
$$

Here A_{ag} and A_{al} are the activities of species a, and A_{wg} and A_{wl} are the activities of species w, in gas and liquid phases, respectively, σ is the surface tension of the cluster, and $X=i/(i+j)$ is the mole fraction of a in the cluster. For the physicochemical data used in our calculations we refer to Refs. 14 and 15. The numerical calculations with the saddle point integration method were performed in the same way as reported by Kulmala and Laaksonen.[14]

The computer program for the exact method was checked by closing the matrix, i.e., setting $e_w=0$ for clusters with m water molecules and $e_a=0$ for clusters with n acid (or ammonia) molecules. As expected, the program produced the equilibrium concentration distribution (4) in these circumstances.

In numerical simulations we have seen that the matrix method approaches correctly to one component limit.

A. Water–sulphuric acid system

For simplicity we did not allow for sulphuric acid hydration in the gas phase. This is not expected to affect the results concerning differences between the exact method and the saddle point integration method.

The upper limits for the numbers of molecules in supercritical clusters (i.e., the matrix size in the exact method) were set to be $n=20$ for sulphuric acid and $m=60$ for water. To make sure that the limits were large enough the nucle-

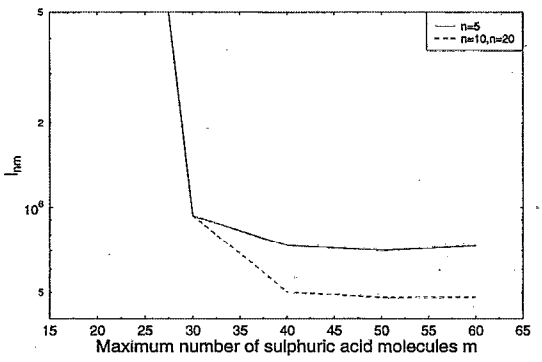

FIG. 2. The number of clusters flowing out of the system in unit time I_{nm} with different upper limits m and n for water and sulphuric acid molecules in a cluster, respectively. The temperature is 233.15 K, the gas phase activity of water is 0.3 and the gas phase activity of sulphuric acid is 10^{-3}.

ation rate was calculated also with $n=80$ and $m=180$. It was also noted that rates started to rise substantially when n was set below 10 and m below 50 (see Fig. 2).

The nucleation rates and saddle point flow directions calculated using both methods are listed in Table I together with saddle point coordinates at different temperatures and gas phase activities. The nucleation rates given by the exact method and the saddle point integration method are always within the same order of magnitude. This shows that the traditional method describes the kinetics accurately enough to be used in large models, where the matrix method is not suitable due to the considerable computational effort needed.

The integral method for the saddle point flow direction is not reasonable, when the saddle point is in the immediate vicinity of the origin. Large differences can be seen in flow directions given by the two methods when the number of molecules in the critical cluster is below about 10; at larger cluster sizes the differences decrease, as expected. The differences in flow directions seen here are estimated to produce maximally a one order of magnitude difference in nucleation rate.

Figure 3 shows the Gibbs free energy surface and Fig. 4 the corresponding steady-state concentrations at 233.15 K, with gas phase activities of 0.3 and 10^{-3} for water and sulphuric acid, respectively. The saddle point is on the middle of the ridge of maximal concentrations in Fig. 4; however, the "ΔG-valley" in Fig. 3 does not appear very steep in the vicinity of the saddle point. Figure 5 shows the steady-state net flows in the same conditions. The arrow lengths are proportional to the logarithms of the flows. Interestingly, negative net flows appear near the origin, creating "current loops." As can be suspected from Fig. 3, substantial net flows can be seen going past the saddle point. This is somewhat surprising considering the relative accuracy of the nucleation rate predictions produced by the saddle point integration method, which assumes that the net flow to stable cluster sizes is dominated by the saddle point contribution.

Note that Fig. 5 shows net flows in the direction of in-

TABLE I. The nucleation rates evaluated with integral method I_k and matrix method I_m and the saddle point flow directions evaluated by integral method ϕ_k and matrix method ϕ_m, the ratios of nucleation rates I_k/I_m, and the coordinates of the saddle points (i^*,j^*) in H_2O–H_2SO_4 system with temperature T, gas phase activity of water S_w, and gas phase activity of sulphuric acid S_a.

T (K)	S_a	S_w	I_k 1/m^3 s	I_m 1/m^3 s	I_k/I_m	i^*,j^*	ϕ_k (°)	ϕ_m (°)
213.15	10^{-1}	0.3	0.25×10^{14}	0.65×10^{14}	0.38	2,4	73.2	41.7
233.15	10^{-1}	0.3	0.40×10^{16}	0.61×10^{16}	0.66	2,3	67.1	57.0
253.15	10^{-1}	0.3	0.83×10^{17}	0.23×10^{18}	0.36	3,6	70.5	50.2
273.15	10^{-1}	0.3	0.12×10^{19}	0.44×10^{19}	0.27	5,3	58.8	89.9
213.15	10^{-1}	0.9	0.57×10^{14}	0.17×10^{16}	0.03	1,1	···	58.8
233.15	10^{-1}	0.9	0.23×10^{17}	0.44×10^{18}	0.05	1,1	···	49.4
253.15	10^{-1}	0.9	0.18×10^{20}	0.41×10^{20}	0.44	2,5	75.8	53.4
273.15	10^{-1}	0.9	0.63×10^{21}	0.19×10^{22}	0.33	2,5	75.7	51.6
293.15	10^{-1}	0.9	0.14×10^{23}	0.60×10^{23}	0.23	2,4	72.4	66.0
213.15	10^{-2}	0.3	0.57×10^{11}	0.14×10^{12}	0.41	2,4	74.0	37.8
233.15	10^{-2}	0.3	0.11×10^{13}	0.30×10^{13}	0.37	3,6	71.2	55.7
253.15	10^{-2}	0.3	0.73×10^{13}	0.17×10^{14}	0.43	5,11	70.9	65.1
273.15	10^{-2}	0.3	0.14×10^{14}	0.36×10^{14}	0.39	6,13	70.2	67.6
213.15	10^{-2}	0.9	0.13×10^{14}	0.24×10^{14}	0.54	2,5	76.7	62.9
233.15	10^{-2}	0.9	0.79×10^{15}	0.25×10^{16}	0.32	2,5	76.6	54.7
253.15	10^{-2}	0.9	0.28×10^{17}	0.11×10^{18}	0.25	2,4	73.9	66.1
273.15	10^{-2}	0.9	0.95×10^{18}	0.26×10^{19}	0.37	3,8	75.6	66.7
213.15	10^{-3}	0.3	0.15×10^{8}	0.41×10^{8}	0.37	3,6	71.9	64.8
233.15	10^{-3}	0.3	0.18×10^{8}	0.48×10^{8}	0.38	5,12	72.5	63.8
253.15	10^{-3}	0.3	0.18×10^{7}	0.44×10^{7}	0.41	8,20	72.5	69.9
213.15	10^{-3}	0.9	0.26×10^{11}	0.84×10^{11}	0.31	2,5	77.3	59.8
233.15	10^{-3}	0.9	0.17×10^{13}	0.30×10^{13}	0.57	3,9	79.6	64.1
253.15	10^{-3}	0.9	0.13×10^{14}	0.37×10^{14}	0.35	3,8	75.9	67.6
273.15	10^{-3}	0.9	0.94×10^{14}	0.23×10^{15}	0.41	4,12	77.5	70.2
213.15	10^{-4}	0.3	0.19×10^{3}	0.53×10^{3}	0.36	5,13	73.8	66.8
213.15	10^{-4}	0.9	0.45×10^{8}	0.84×10^{8}	0.54	3,10	80.0	60.5
233.15	10^{-4}	0.9	0.14×10^{9}	0.46×10^{9}	0.30	4,13	76.2	70.8
213.15	10^{-5}	0.9	0.10×10^{5}	0.13×10^{5}	0.77	4,14	82.5	71.0

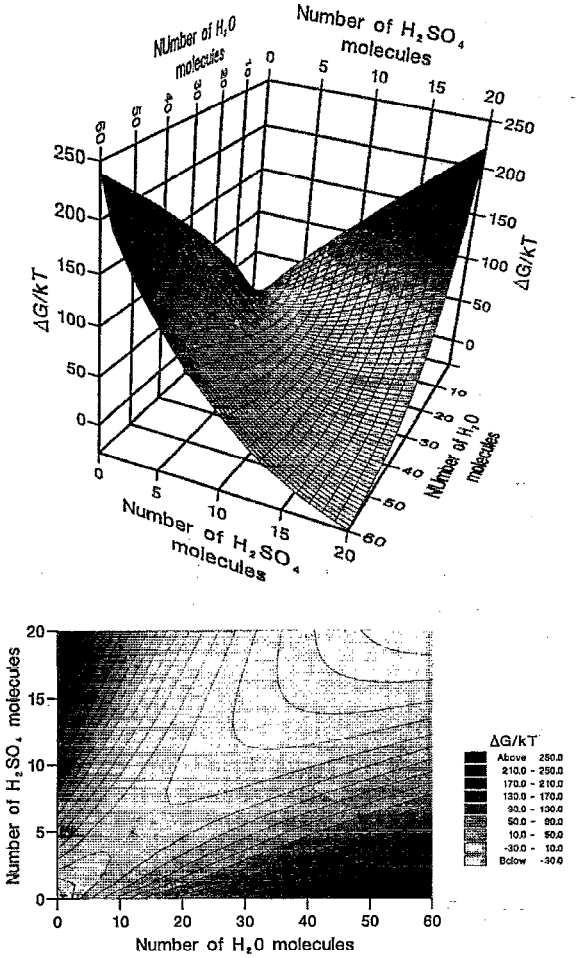

FIG. 3. The Gibbs free-energy (per kT) of formation of the cluster in the H_2O–H_2SO_4-system at 233.15 K with gas phase activity of H_2O 0.3 and gas phase activity of H_2SO_4 10^{-3}. The saddle point is marked with an asterisk.

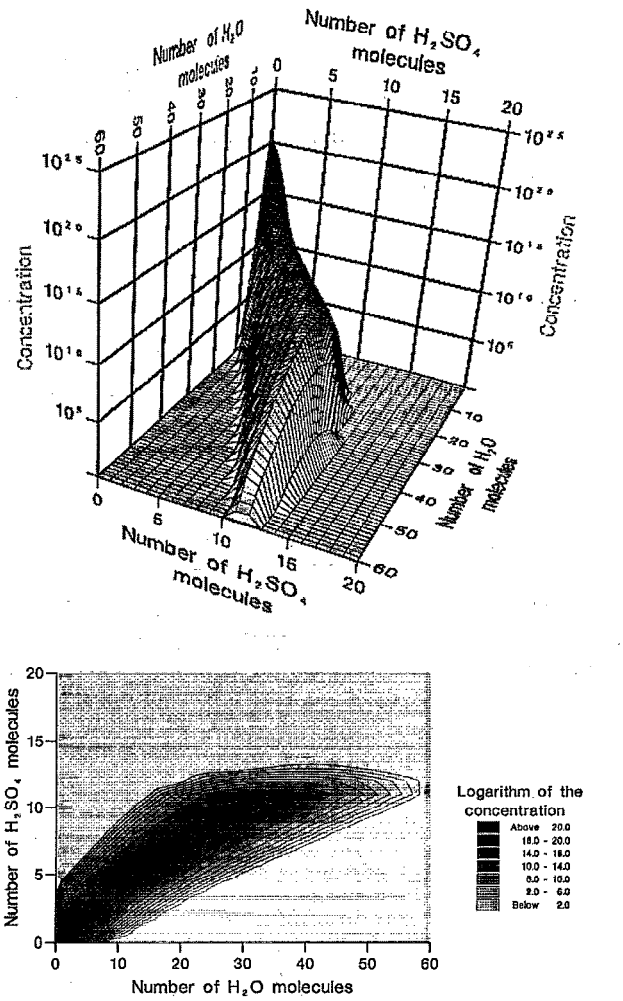

FIG. 4. Steady-state concentrations (per m^{-3}) in the H_2O–H_2SO_4-system at 233.15 K with H_2O gas phase activity of 0.3 and H_2SO_4 gas phase activity of 10^{-3}. The location of the saddle point in Gibbs free-energy surface is marked with an asterisk. For graphical reasons, concentrations below 1 particle/m^3 are not shown.

creasing numbers of both water and sulphuric acid molecules. This indicates that the approximation of flows in water direction being zero, which has sometimes been used in the literature, is not valid.

The total number concentration of both water and acid molecules bounded in clusters can be evaluated from the steady-state concentration distribution. It is seen that the monomer concentration of water is higher than the concentration of bounded water molecules, but this does hold for sulphuric acid molecules. This, in fact, means that the steady state approximation is very questionable in the case of binary water–sulphuric acid nucleation.

B. Water–ammonia system

The upper limits of numbers both water and ammonia molecules in one cluster, m and n, were set to be 50, and the calculations were repeated with $m=n=60$. As with sulphuric acid, the nucleation rates calculated with too low limits were found to be too high.

Nucleation rates, saddle point coordinates, and flow directions calculated with both methods are shown in Table II. The saddle point flow directions match quite well, but the nucleation rates given by different methods differ approxi-

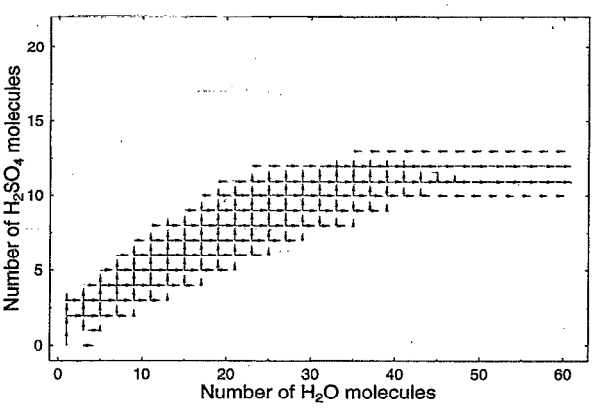

FIG. 5. Steady-state flows in the H_2O–H_2SO_4-system at 233.15 K with H_2O gas phase activity of 0.3 and H_2SO_4 gas phase activity of 10^{-3}. The arrow length is proportional to the logarithm of the flow. Flows below 3/m^3 s are not shown. For clarity, we show flows only from cluster sizes containing an odd number of water molecules.

TABLE II. The nucleation rates evaluated with integral method I_k and matrix method I_m and the saddle point flow directions evaluated by a integral method ϕ_k and matrix method ϕ_m, the ratios of nucleation rates I_k/I_m, and the coordinates of the saddle points (i^*,j^*) in H_2O–NH_3 system with temperature T, gas phase activity of water S_w and gas phase activity of ammonia S_a.

T (K)	S_a	S_w	I_k 1/m^3 s	I_m 1/m^3 s	I_k/I_m	i^*,j^*	ϕ_k (°)	ϕ_m (°)
233.15	0.31	2.5	0.84×10^{16}	0.38×10^{13}	2.2×10^{3}	35,20	75.5	76.0
233.15	0.23	3.0	0.16×10^{17}	0.46×10^{13}	3.5×10^{3}	36,18	77.6	80.9
233.15	0.16	3.5	0.75×10^{16}	0.31×10^{13}	2.4×10^{3}	37,15	80.4	84.4
223.15	0.45	2.5	0.23×10^{17}	0.12×10^{14}	1.9×10^{3}	29,18	75.5	71.5
223.15	0.33	3.0	0.20×10^{17}	0.10×10^{14}	2.0×10^{3}	30,16	77.7	78.1
223.15	0.25	3.5	0.26×10^{17}	0.12×10^{14}	2.2×10^{3}	31,15	79.0	81.6
223.15	0.19	4.0	0.28×10^{17}	0.13×10^{14}	2.2×10^{3}	30,13	80.5	84.3
223.15	0.14	4.5	0.20×10^{17}	0.86×10^{13}	2.3×10^{3}	31,12	81.5	86.0
223.15	0.11	5.0	0.32×10^{17}	0.12×10^{14}	2.7×10^{3}	31,11	82.1	87.0

mately by a factor 2×10^3. One reason for the difference may be that the Gibbs free energy surface is quite flat compared with e.g. the water–sulphuric acid case. Figure 6 shows the steady state net flows at 223.15 K with gas phase activities 4.0 and 0.19 for water and ammonia, respectively. According to Wu,[16] another possible contribution to the difference stems from the fact that Stauffer's[1] integration of the nucleation rate incorporates contributions from unphysical negative cluster sizes.

IV. CONCLUSIONS

The matrix method presented in this paper describes the binary nucleation kinetics exactly. The method is independent of the way of obtaining evaporation coefficients. Using the same equations in nonsteady state situations and solving the differential equations one would be able to work out the time lag for binary homogeneous nucleation (see Ref. 17).

The conventionally used theory approximates well the nucleation rates in water–sulphuric acid systems. In water–ammonia systems there is an approximately constant difference of the order of 10^3 between the nucleation rates calculated with the exact method and Stauffer's saddle point integration method. The saddle point flow directions given by Stauffer's method are better approximations to the exact results in water–ammonia system than in water sulphuric acid system.

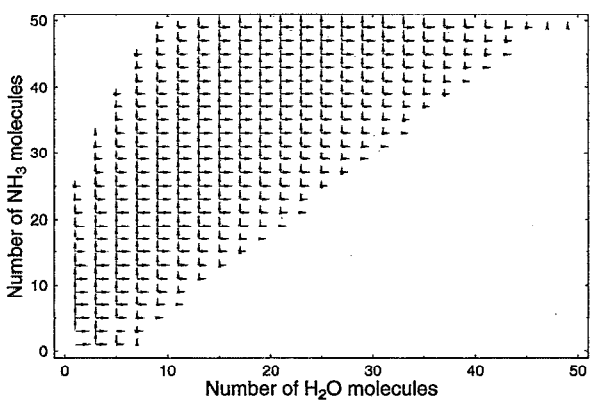

FIG. 6. Steady-state flows in the H_2O–NH_3-system at 223.15 K with H_2O gas phase activity of 4.0 and NH_3 gas phase activity of 0.19. The arrow length is proportional to the logarithm of the flow. Flows below 3/m^3 s are not shown. For clarity, we show flows only from cluster sizes containing an odd number of water molecules.

ACKNOWLEDGMENT

Support of this work by the Academy of Finland is gratefully acknowledged.

[1] D. Stauffer, J. Aerosol Sci. **7**, 319 (1976).
[2] J. E. McDonald, Am. J. Phys. **31**, 31 (1963).
[3] G. J. Doyle, J. Chem. Phys. **35**, 795 (1961).
[4] H. Reiss, J. Chem. Phys. **18**, 840 (1950).
[5] R. H. Heist and H. Reiss, J. Phys. Chem. **61**, 573 (1974).
[6] A. Jaecker-Voirol and P. Mirabel, J. Phys. Chem. **92**, 3518 (1988).
[7] C. S. Kiang and D. Stauffer, Faraday Symp. Chem. Soc. **7**, 26 (1973).
[8] M. Kulmala, A. Laaksonen, and S. L. Girshick, J. Aerosol Sci. **23**, 309 (1992).
[9] G. Wilemski, J. Chem. Phys. **80**, 1370 (1984).
[10] A. Laaksonen, M. Kulmala, and P. Wagner, J. Chem. Phys. **99**, 6832 (1993).
[11] S. K. Friedlander, *Smoke, Dust and Haze* (Wiley, New York, 1977).
[12] B. Nowakowski and E. Ruckenstein, J. Phys. Chem. **96**, 2313 (1992).
[13] FORTRAN-routine F07BEF. *The NAG Fortran Library Manual. Mark 15* (The Numerical Algorithms Group, Oxford, 1991), Vol. 6.
[14] M. Kulmala and A. Laaksonen, J. Chem. Phys. **93**, 696 (1990).
[15] T. Vesala and J. Kukkonen, Atmos. Environ. **26A**, 1573 (1992).
[16] D. T. Wu, presented at the 68th Annual Colloid and Surface Science Symposium, Stanford University, 1994 (unpublished).
[17] K. Nishioka and K. Fujita, J. Chem. Phys. **100**, 532 (1994).